Challenges in Snow and Ice Albedo Parameterizations

Roberta Pirazzini

Finnish Meteorological Institute, P.O. Box 503, FIN-00101 Helsinki, Finland

Abstract

The surface albedo in snow-covered regions is a critical factor controlling climate sensitivity. However, still large uncertainty characterizes the present-day simulation of the snow albedo. This paper summarizes the physical and modeling challenges in deriving snow and ice albedo parameterizations, briefly presenting the state of art of the existing parameterizations and evidencing also the effects of model structure and other model's parameterizations on the albedo result. A general recommendation to improve the snow and ice albedo parameterization is to develop more physically-based schemes. To reach this objective, it is of paramount importance to carry out field experiments with simultaneous measurements of albedo and snow properties (snow grain size and density, vertically resolved temperature, impurity concentration) at high temporal resolution.

Key words: snow, ice, albedo parameterization, modeling of polar climate

1. Introduction

Under clear skies, the diffuse radiation reflected by a snow/ice surface is not isotropic, but it is distributed according to the bidirectional reflectance distribution function, which is the ratio between the reflected radiance and the incident radiance projected along the vertical to the surface (*Warren*, 1982). The spectral albedo α_λ is the 'spectral directional-hemispherical reflectance', i.e. the integral of the bidirectional reflectance distribution function over all reflection angles:

$$\alpha_\lambda = \int_0^1 \mu' d\mu' \int_0^{2\pi} \frac{dI}{\mu_0 dF} d\phi' \tag{1}$$

where μ_0 is the cosine of the incident zenith angle, μ' the cosine of the reflected zenith angle, ϕ' the reflected azimuth angle, λ the wavelength, F the incident irradiance (on a surface normal to the beam), and I the reflected radiance. In other words, the spectral albedo is the upward shortwave irradiance divided by the downward shortwave irradiance at a particular wavelength. The spectrally integrated albedo is found from integrating equation (1) over the solar spectrum.

Equation (1) employed in the radiative transfer schemes, defines the albedo as an apparent optical property of the surface, although it still depends on the solar direction (it is also called "black-sky albedo"). However, the observed albedo depends also on the atmospheric properties (including clouds), because of the atmospheric multiple scattering and absorption effects (due, above all, to aerosols and water vapour molecules). Thus, the spectrally integrated albedo α_s measured by pyranometers over a snow surface corresponds to the weighted sum of the "black-sky albedo" (associated with the direct irradiance) and the "white-sky albedo" (associated with the diffuse irradiance), and is obtained from the ratio

$$\alpha_s = \frac{Sw_\uparrow}{Sw_\downarrow} \qquad\qquad\qquad (2)$$

where $Sw_\uparrow$ and $Sw_\downarrow$ are the measured upward and downward shortwave irradiances, respectively.

Polar Regions are characterized by the largest albedo contrasts at the surface, due to the proximity and seasonal alternation of snow covered areas and bare ground or water surfaces. Also, snow and ice albedo themselves undergo large variations during the melting and freezing/accumulation periods. Since surface albedo controls the amount of solar radiation absorbed at the surface, an incorrect representation of the snow albedo and the snow cover fraction (f_s) causes large errors in the weather forecast and in the simulations of the present-day and future climate at high latitudes. Indeed, climate models have much more pronounced systematic present-day albedo biases over snow-covered than over snow-free areas (*Roesch*, 2006), and the largest intermodal scatter in CO2-induced warming occurs at high latitudes (*Bony et al.*, 2006).

Several recent studies have demonstrated that surface albedo in snow-covered regions is a critical factor controlling climate sensitivity (*Levis et al.*, 2007, *Qu and Hall*, 2007). The positive feedback of the snow- and ice-albedo on temperature (also called albedo-temperature feedback) is an important factor contributing to the high-latitude amplification of the global warming (*Robock*, 1983; *Hall*, 2004). The large intermodel variation of the strength of the snow-albedo feedback in the future climate scenario is very much correlated with the intermodel differences in albedo sensitivity to the air temperature in the present day climate (*Hall and Qu*, 2006). Thus, the correct simulation of the present-day snow albedo is a fundamental prerequisite for a realistic prediction of the future climate. However, still large uncertainty characterizes the present-day simulation of the snow albedo and its impact on present-day climate. For instance, the positive multidecal correlation between the increase in spring land temperature and the reduction of snow cover in the Northern Hemisphere shown by the observations is not reproduced by many climate models (*Roesch*, 2006).

In most climate and Numerical Weather Prediction (NWP) models, the interaction of snow and ice with the atmosphere is poorly represented, as models are tailored for low and middle latitudes where the presence of snow and ice is much less significant than close to the Poles. In particular, the model representation of the snow and ice

albedo is one of the most serious oversimplifications, causing large errors in weather prediction and climate simulations (*Curry et al.*, 2001; *Pirazzini et al.*, 2002; *Liu et al.*, 2007). On the other hand, accurate snow physical schemes that consider snow grain size (*r*) and crystal structure and are based on the radiative transfer theory, work only on single column experiments, because they are computationally intense, and cannot account for the large horizontal variability of snow microphysical and macrophysical properties. Thus, in climate and NWP models, albedo has to be represented by parameterizations that are simple and fast enough, but that also take into account all the relevant physical processes that concur in affecting the albedo.

The sea ice albedo depends on snow thickness, melt pond fraction, brine volume and air bubbles (*Grenfell and Maykut*, 1977). The snow albedo decreases when snow ages, as grains become more rounded and increase in size. Snow metamorphism, which very much shapes the temporal albedo evolution, includes three main processes: destructive or equi-temperature metamorphism, temperature-gradient metamorphism and melt metamorphism. Temperature-gradient and melt metamorphisms depend on the temperature and the temperature history: during melting the growth of the snow grains is rather fast, and the presence of melted water between the grains further decreases the albedo. Fresh snow is usually highly faceted and reflective, but also its albedo may vary a lot depending on the wetness of the grains. As the snow albedo decreases, the penetration depth of light increases, and the surface albedo is increasingly affected by the reflectivity of the deeper layers. Thus, the surface albedo depends very much on the snow depth (h_s), especially when it is lower than 0.1 m (*Grenfell and Perovich*, 2004). The presence of impurities in the snow such as soot and ash can decrease the albedo, depending on *r* and on the concentration of impurities (*Warren*, 1982).

Snow and ice albedo increase with increasing solar zenith angle (θ), especially when the grains at the surface are faceted, as the light incident at lower angles penetrates deeper into the snowpack and is more likely trapped. Albedo also increases with increasing cloud cover, as the ratio of diffuse to global radiation increases (although this increases the albedo only for $\theta < 70°$) and the incoming radiation flux becomes richer in the visible spectrum, for which snow albedo is higher than in the near-infrared region. Wind may have opposite effects on snow albedo, depending on atmospheric conditions (temperature and humidity): it may increase the albedo by breaking the fresh snow crystals and leading to the formation of a surface layer of small, highly faceted ice needles, or it may decrease it by compacting the surface layers of snow and thus increasing the snow density (ρ_s) and bonds.

Although the various mechanisms affecting the snow and ice albedo are known, their relative importance is not clearly assessed, and the wide variety of existing albedo parameterizations derives from the different attempts to account for the most relevant factors driving the albedo evolution. In most Land Surface Schemes, surface albedo is function of both snow albedo and f_s. Thus, it is the combination of the parameterizations of snow albedo and f_s that mostly affects the modeled grid cell albedo.

Tens (or hundreds) of parameterizations for snow and ice albedo have been developed, with various degrees of complexity. The aim of this work is to summarize

the physical and modeling challenges in deriving snow and ice albedo parameterizations, to briefly present the state of art of the existing parameterizations, to evidence the effect of model structure and other model's parameterizations on the albedo result, and to identify some strategies for the future observational campaigns and modeling development. The paper is organized as follows. Section two summarizes the main inherent physical problems that make the development of snow and ice albedo parameterizations particularly difficult. Section three addresses the handling of the spatial albedo heterogeneity in models, and the parameterization of f_s. Section four reviews the present day snow and ice albedo schemes, describing in the last subsection some aspects that should possibly be addressed in the future development of the albedo parameterizations. Section five describes the most important model aspects that are not related to the albedo parameterization but still affect the albedo simulation. Section six discusses some of the significant impacts of the albedo parameterizations on the future climate simulations. Finally a conclusion section follows.

2.   *Inherent difficulties in producing albedo parameterizations*

A first problem arises from the fact that the parameters that are found to significantly affect the snow albedo are different in different sites (*Pedersen and Winther*, 2005). Moreover, no parameterization scheme performs consistently better than the other schemes in every season and year, even at a single site. This is probably because the schemes have different sensitivities to the parameters (Table 1), which have a different impact on the albedo depending on the weather and the precipitation history (*Pedersen and Winther*, 2005). Because of differences in the local weather regimes (precipitation, temperature, insolation, wind exposure) and in the type of underlying surface, different parameterizations work better in different seasons, different latitudes, and different years.

Snow water equivalent (SWE) is a prognostic variable in most snow schemes, but it has large differences among models, due to inaccuracies in the modeled precipitation and to the different approximations made to represent the snow-scheme and the turbulent transfer at the surface (*Loth and Graf*, 1998; *Boone and Etchevers*, 2001). Indeed, uncertainty on precipitation (modeled but also measured) is considered one of the biggest sources of error in albedo parameterizations (*Zuo and Oerlemans*, 1996). For instance, a very light snowfall is extremely difficult to forecast by atmospheric models and it is also challenging for measuring, but it may dramatically raise the surface albedo (*Greuell and Konzelmann*, 1994; *Grenfell and Perovich*, 2004; *Pirazzini et al.*, 2006).

Generally, the parameterizations are based on observational datasets, and they include empiric parameters that are characteristic of the albedo variability of that specific dataset. The most important of these parameters are the maximum and minimum allowed albedo. It is obvious that especially the minimum albedo can vary a lot depending on the underlying surface. Many snow and ice albedo parameterizations have ice albedo minima around 0.5, as they are mostly tailored for the Arctic, where the average ice thickness is few meters. These parameterizations are not suitable for

relatively thin sea ice (less than a meter thick), as for instance can be found in spring in the Baltic Sea. Over a 30 cm-thick ice in the Gulf of Finland the recorded bare ice albedo was between 0.15 and 0.3 (*Rasmus et al.*, 2002). Moreover, the maximum prescribed snow albedo is usually between 0.8 and 0.85, but the observed albedo of fresh snow can reach up to 0.95.

Table 1. Parameters that are found to be significantly affecting the daily mean snow albedo (X is significant at the 95% confidence level) in different sites: surface temperature (T), cloud cover fraction (N), wind speed (WS), h_s, positive accumulated degrees days (ACC), and days after snowfall (Age). Data are from *Brock et al.* (2000), *Pedersen and Winther* (2005), and *Mölders et al.* (2007). Not calculated dependencies are marked with Nc.

Measurement sites	T	N	WS	h_s	ACC	Age
Ny-Ålesund (78.9°N, 11.9°E) *Svalbard, Norway*	X			X	X	Nc
Col de Porte (1340m a.s.l., 45.3°N, 5.8°E) *France*	X	X		X	X	Nc
Uralsk (51.3°N, 51.4°E) *Russia*	X	X		X	X	Nc
Tulun (490m a.s.l., 54.6°N, 100.6°E) *Russia*	X		X	X		Nc
Barrow (71.3°N,156.78°W) *Alaska, U.S.*	X		X	X		X
Haut Glacier d'Arolla (2572-3002m a.s.l., 46.0°N, 7.5°E) *Switzerland*	Nc	Nc	Nc	X	X	X

The snow masking over vegetation and forests is particularly difficult to model. *Rutter et al.* (2009) compared thirty-three snowpack models of varying complexity, concluding that there was not a universal "best" model, and that most challenging was the simulation of SWE over forested sites. Different models performed better in different sites, and, at a single site, different models performed better in different years. Indeed, the largest differences in surface albedo among the IPCC-AR4 models (see list of acronyms for explanation) are found over snow-covered forested regions (*Roesch*, 2006), with most of the models predicting positive albedo biases. These problems have a strong impact also on the performance of NWP models: *Viterbo and Betts* (1999) showed that a reduction of the deep snow albedo in boreal forest from 0.8 to 0.2 in ECMWF model reduced the systematic cold temperature bias in the lower troposphere at high northern latitudes during spring.

3.   *Handling of spatial albedo heterogeneity*

Investigating the sub-grid variability of the albedo, *Roesch et al.*, (2004) demonstrated that ignoring information about intra-cell variance may lead to significant errors in the simulated regional climate and horizontal fluxes, particularly in orographically rough and snow-covered areas. Many of the modern surface schemes used in weather forecast and climate models can account for various surface types (tiles)

inside a grid-cell (for instance BATS (*Dickinson et al*, 1993), CLM (*Oleson et al.*, 2004), and ISBA (*Douville et al.*, 1995)). The grid cell albedo is generally obtained from the weighted average of the albedo of the various tiles. In case of strong albedo contrasts among the tiles, as for instance in case of water and snow surfaces, the weighted average of the tiles' albedo gives a correct quantification of the grid cell albedo under cloudy skies only in case of small scale heterogeneity (few meters to few hundreds of meters), as it is for the melt ponds in the Arctic (*Benner et al.*, 2001; *Barker et al.*, 2002). For larger scale surface heterogeneities, which could be found in grid cells including coastlines or the margin between forests and snow-covered fields, the weighted average of the tiles' albedo most probably produces an underestimation of the effective albedo of the grid cell and of the downelling shortwave radiation, because of the radiative interaction between the surface and the cloud base (*Pirazzini and Räisänen*, 2008).

f_s inside a grid cell is often parameterized as a function of SWE (i.e. in ISBA) or h_s, which is however diagnostically derived from SWE and from the parameterized ρ_s (i.e. in CLM and BATS). *Yang et al.* (1997) introduced a parameterization which accounts for the two distinct stages in the f_s - h_s relationship: a fist stage where f_s (and surface albedo) increases sharply as h_s increases until a critical depth, and a second stage where f_s (and snow albedo) shows a very slow increase with h_s once the critical depth is reached. *Niu and Yang* (2007) further developed this parameterization by adding a dependence on ρ_s, to account for the variation of the f_s - h_s relationship with season (the increase of f_s with h_s in autumn is more rapid than the decrease of f_s with h_s during the spring melting period).

The parameterization of f_s has a large impact on the grid cell albedo. Studying the model sensitivity of the f_s parameterization, *Levis et al.* (2007) showed that using parameterizations that generate larger f_s and faster increase of f_s with SWE leads to higher surface albedo, lower surface temperature, stronger surface albedo feedback on the temperature, and enhanced global warming in case of doubling the CO_2. *Roesch* (2006) observed that most ICCP-AR4 models overestimate SWE in spring. However, this overestimation is not necessarily related to positive f_s anomalies, since the relationship between SWE and f_s is highly nonlinear. Indeed, f_s is extremely sensitive to SWE changes in thin snowpack, while it is almost insensitive to SWE changes for thick snowpack. Moreover, positive biases in snow cover area are not necessarily related to positive albedo biases (*Roesch*, 2006). This conclusion points out the importance of a correct parameterization of the snow albedo itself, in addition to the f_s, for a reasonable representation of the surface albedo.

4.   *Parameterizations of snow and ice albedo*

The role of the albedo parameterization is critical in the performance of both NWP models and climate models. *Lynch et al.* (1998) showed that the choice of a particular snow-albedo formulation has a dominant impact on the speed of the snowmelt in spring, with profound consequences on the climate due to the numerous feedback

mechanisms involving a large change in albedo. Analyzing a case study over sea ice in the Baltic Sea, *Pirazzini et al*. (2002) showed that when fresh snow was present at the surface, the HIRLAM underestimation of the sea ice albedo (which had a maximum value of 0.7 in the HIRLAM version 4.6.2) and the erroneous setting of the snow thermodynamic parameters to the values proper for old snow, produced a delay in the surface cooling and about 3°C of error in the surface temperature in the 6-hour forecast. *Køltzow* (2007) showed that improving the description of snow and sea ice albedo in the climate model HIRHAM (adding for instance the effect of melt ponds) significantly improved the model performance in spring, reducing of 2–3°C the temperature bias (of 5–6°C) that HIRHAM originally had compared to the ERA40 reanalysis products. Moreover, the new parameterization reduced the mean sea level pressure bias (strengthening the low pressure system) compared to ERA40 during spring and autumn. *Køltzow* (2007) also concluded that, due to the sea ice albedo feedback processes, the sensitivity to the albedo parameterization would be even higher in coupled climate models.

Several snow/ice albedo parameterizations have been developed, with various degrees of complexity. Table 2 lists the parameterizations of snow/ice albedo and f_s used in various models cited in this section. The table includes land surface schemes (BATS, LSM, CLM, ISBA), a NWP model (ECMWF), atmospheric climate models (ECHAM4, ECHAM5, CAM2), and coupled climate models (HadCM3). The simplest parameterization schemes apply two or more constant values of albedo for different surface types (for example the HIRLAM model version 4.6.2 applied in *Pirazzini et al*. (2002)). Other schemes add a dependence on temperature (for example ECHAM4 and ECHAM5) when the surface approaches the melting point, to account for the combined effects of snow metamorphism and snow thinning. More sophisticated schemes also include the albedo dependence on snowfall occurrence (for example ISBA), snow/ice thickness and θ (for example BATS and LSM).

Table 2. Description of the models commented in the text and details of their snow/ice albedo schemes.

Model	Snow/ice albedo scheme	Snow cover fraction
BATS (*Dickinson et al*, 1993; *Lynch et al*., 1998) Land surface model designed for coupling with various NCAR GCM.	For diffuse radition: α_s is a linear function of *Age* For direct radiation: α_s is a linear function of *Age* and non-linear function of μ. Different coefficients are applied depending on whether visible (*vis*) or near-infrared (*nir*) waveband is being considered. $\alpha_{i,vis}$ =0.80 and $\alpha_{i,nir}$ =0.6.	$f_s = \dfrac{F_{sn}}{1+F_{sn}}$ $F_{sn} = h_s \dfrac{0.1}{z}$ $\rho_s = \rho_{snew} \cdot \left(1 + \dfrac{3Age}{1+Age}\right)$ ρ_{snew} = 100 kg m^{-3}
CAM2 (*Collins et al*., 2002) NCAR Atmospheric GCM	α_s depends on the waveband (*vis* and *nir*) and is a linear function of T between -1°C and 0°C. For $T < $ -1°C $\alpha_{s,vis,\max}$ = 0.98 and $\alpha_{i,vis,\max}$ =0.78, while $\alpha_{s,nir,\max}$ = 0.70 and $\alpha_{i,nir,\max}$ 0.36. For T =0°C $\alpha_{vis,\min}$ =0.88, $\alpha_{nir,\min}$ =0.55, while α_i decreases linearly with temperature.	$f_s = \dfrac{h_s}{h_n + 0.02}$

Model	Albedo parameterization	Fractional snow cover
CLM (*Oleson et al., 2004*) Land surface model developed from the merging of BATS and LSM for coupling to the CCSM.	α_s is taken from BATS, while α_i is taken from LSM.	$f_s = \dfrac{h_s}{h_s + z}$
ECHAM4 (*Roeckner et al.*, 1996; *Roesch et al.*, 1999) Atmospheric GCM of the Max Planck Institute for Meteorology, Hamburg, Germany	α_s is linear function of surface temperature T between -10°C and 0°C. For $T < $ -10°C α_{max} = 0.75, 0.8, 0.8, 0.4 for sea ice, land ice, snow on forest-free land, snow on forested land. For $T = 0$°C α_{min} =0.5, 0.6, 0.4, 0.3 for sea ice, land ice, snow on forest-free land, snow on forested land.	$f_s = \dfrac{S_n}{S_n + 0.01}$
ECHAM5 (*Roeckner et al.*, 2003) Atmospheric GCM of the Max Planck Institute for Meteorology, Hamburg, Germany	α_s is linear function of surface temperature T between -5°C and 0°C. For $T < $ -5°C α_{max} = 0.75, 0.8, 0.8, 0.2 for sea ice, land ice, snow on forest-free land, snow on forested land. For $T = 0$°C α_{min} =0.5, 0.6, 0.3, 0.2 for sea ice, land ice, snow on forest-free land, snow on forested land.	f_s = tanh function of S_n and slope terrain
ECMWF (*ECMWF*, 2007; *Douville*, 1995; *Van den Hurk and Viterbo*, 2003) European medium-range weather forecast model.	α_s is expressed by a prognostic equation with linear decrease with time for $T < 0$°C, and exponential decrease with time for $T = 0$°C. For $T < 0$°C the slope of the decrease depends on T. $\alpha_{s,min}$ =0.5 and $\alpha_{s,max}$ =0.85. The maximum value is applied whenever a snowfall exceeds the threshold value of 1 mm/h. α_i is derived from a monthly climatology (Los et al., 2000).	f_s = linear function of S_n for $S_n<0.115$ m, f_s =1 elsewhere.
HadCM3 (*Cox et al.*, 1999; *Gordon et al.*, 2000) Climate Model produced by the Hadley Centre for Climate Prediction and Research, Met Office, United Kingdom.	For deep-snow, when $T \leq 2$°C α_s is equal to a prescribed value which depends of the land cover class, while when $T > 2$°C α_s decreases linearly with T. For intermediate snow depths, the grid box albedo approaches the deep-snow value exponentially, according to an e-folding depth of snow equivalent to 5 mm of water. α_i is 0.80 for $T < $ -10°C and decreases linearly from 0.80 and 0.50 when $T > $ -10°C.	Implicitly parameterized in the albedo formulation for intermediate snow depths.
ISBA (*Douville et al.*, 1995) Land-surface scheme implemented into the Météo-France climate and weather prediction model ARPEGE, and into the weather prediction model HIRLAM5 (and subsequent versions).	α_s is expresses by a prognostic equation with linear decrease with time for $T < 0$°C, and exponential decrease with time for $T = 0$°C. $\alpha_{s,min}$ =0.5 and $\alpha_{s,max}$ =0.85. The maximum value is applied whenever a snowfall exceeds the threshold value of 10 mm. α_i is derived from the monthly climatology of the ECOCLIMAP database (Masson et al., 2003).	f_s = diagnostic equation as a function of ρ_s, SWE, z and subgrid orography. ρ_s =prognostic equation with exponential increase with time, from $\rho_{s\,min}$ = 100 kg m^{-3} to $\rho_{s\,max}$ = 300 kg m^{-3}.

| LSM 1.0 (*Bonan*, 1996; *Marshall and Oglesby*, 1994)

Land surface model designed for coupling to atmospheric numerical models. It has been incorporated into the CCSM, which also includes oceanic and sea-ice components. | α_s depends on the waveband (*vis* and *nir*), μ, r, T, and soot content.

$\alpha_{i,vis}$ =0.80 and 0.60 for glaciers and frozen lakes, respectively,
$\alpha_{i,nir}$ =0.55 and 0.40 for glaciers and frozen lakes, respectively. | $f_s = \dfrac{h_s}{h_s + z}$

ρ_s= 200 Kg m^{-3}
z = 0.25 m |

4.1   *Temperature-dependent schemes*

Temperature-dependent albedo schemes usually have a minimum and maximum albedo values corresponding, respectively, to melting conditions and to surface temperatures (T) below a certain threshold (which varies among models between -1°C and -10°C). For intermediate T, albedo varies linearly with T or follows a polynomial dependency. In some models a separate dependency on T is prescribed for visible and near-infrared wavelengths (*Roesch et al.*, 2002).

Several observational studies showed indeed this sort of correlation between albedo and T. On the basis of satellite albedo products, *Ross and Walsh* (1987) proposed a parameterization for the sea ice albedo of the Arctic that consisted in a linear albedo decrease for T between -5 and 0°C, with constant albedos of 0.80 and 0.65 for T<-5°C and T=0°C, respectively. Figure 1 shows the Ross and Walsh's parameterization together with daily mean albedo and T obtained from two filed campaigns in the Baltic Sea and in Antarctica. The scattering of data is rather large, especially if also snowfall events are included, however an albedo decline when approaching the melting point can be observed. The strength of the albedo decline depends on the albedo on of the underlying ice, around 0.6 at Hells Gate, in Antarctica, and 0.3 over the Baltic Sea (*Pirazzini*, 2004, *Pirazzini et al.*, 2006). A similar variability in albedo was observed also at four Russian continental stations (*Roesch et al.*, 1999) and in Alps (*Brock at al.*, 2000). These observational analyses seems to suggest that the snow/ice albedo is strongly sensitive to T over those surfaces that are characterized by an alternation of snow and bare ground or thick ice, and are subject to both snowfall and strong melting during the summer. However, the data analyzed over the above cited locations were midday and clear sky albedo observations (*Brock et al.*, 2000), temporally averaged quantities as daily means (Fig. 1) and monthly means (*Roesh et al.*, 1999), and spatially averaged satellite-derived albedo (*Ross and Walsh*, 1987). Therefore, rapid variations in T were smoothed out and the impact of the diurnal oscillation above and below the melting point associated to the freeze-melt cycle was avoided. Moreover, the large scattering of data in Figure 1 indicates that temperature alone is not sufficient to explain the albedo variability.
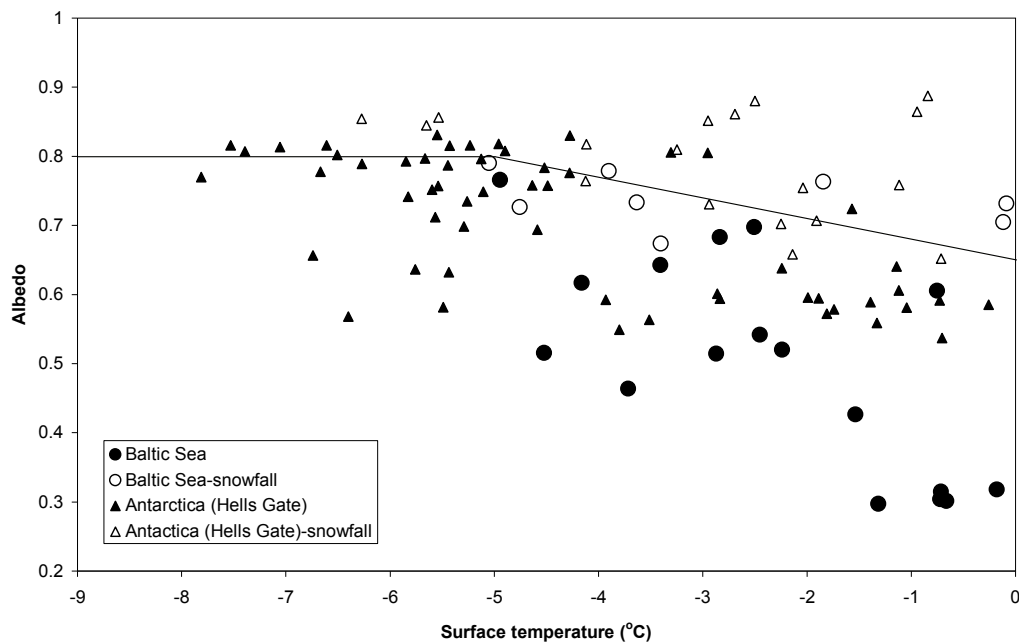
Fig. 1. Daily mean surface albedo versus daily mean surface temperature near Umeå in the Baltic Sea (circles) from 16/3/04 to 10/4/04 and at Hells Gate in Antarctica (triangles) from 5/11/97 to 31/1/98. Empty symbols mark the cases when snowfall occurred. The thick line corresponds to the snow/ice albedo parameterization developed by *Ross and Walsh* (1987).

Calculations based on two decades of satellite observations (1981–2000) revealed that the time-averaged correlation coefficient between clear-sky surface albedo and T varies a lot over the Antarctic continent (*Laine*, 2008). The strongest negative correlation was observed over low wind zones in the plateau and along the highly windy coast, and the weakest correlation in correspondence of moderate-wind areas in the plateau where the katabatic flow originates (*Parish*, 1988). These founding may suggest that moderate and frequent winds ensured a continuous renewal of fine small crystals at the surface, which kept the snow albedo rather unchanged and independent on T.

Comparing several snow albedo schemes based on a temperature dependency, *Køltzow* (2007) concluded that over snow-covered and non-forested area the polynomial approach by *Roesch* (2000) is superior to the other schemes (ECHAM4, ECHAM5, CAM2), as it gave the best performance in spring, when the impact of the snow albedo parameterization on the overall model simulation is largest. Over snow-covered forest, ECHAM5 produced the smallest bias from the observations.

Over sea ice, a frequent deficiency of the T-dependent schemes is that albedo decreases too rapidly at the beginning of the melting season, when T approaches the melting point (*Køltzow*, 2007). In addition, common feature of both T-dependent and more sophisticated T /waveband/snow aging-dependent schemes is a substantial overestimation of the albedo in summer. Comparing SHEBA data of average albedo over a 200-m long line with the albedo simulated using various T-dependent parameterizations, *Køltzow* (2007) observed that the albedo overestimation produced by the models varied between 0.02 and 0.15 in July and between 0.12 and 0.20 in August. The overestimation of the modeled albedo is mainly caused by neglecting the effect of

melt pond formations, and it produced an underestimation of the shortwave radiation absorbed at the surface (between 7 and 44 Wm^{-2} on monthly average). The conclusion was that none of the tested schemes was superior to the others as they fail to describe the annual cycle of albedo. *Køltzow* (2007) proposed then an albedo parameterization that includes the effects of snow and melt ponds on the sea ice, obtaining significant improvement of the model performance in the Central Arctic. However, *Cheng et al.* (2007) demonstrated that Køltzow's parameterization (2007) produces a far too strong and unrealistic albedo response to T when applied to simulate the albedo decay during 2006 spring melting season in the northern edge of the Baltic Sea, where melt ponds are not usually present. Indeed, the T-dependent parameterizations caused unrealistic oscillation between the minimum and maximum albedo values when using the 10-minute time series of observed surface temperature during a spring snowmelt period in the Baltic Sea (*Pirazzini et al.*, 2006). Moreover, the inclusion of the albedo dependence on T may trigger a large amplification of errors when the parameterization is applied in thermodynamic sea ice models to calculate the ice and snow mass balance. When the albedo parameterization is too sensitive to T, errors in the surface energy and mass balance grow rapidly due to the strong positive feedback between albedo and temperature errors (*Cheng et al.*, 2006).

4.2 Comparisons among other albedo schemes

Oerlemans and Knap (1998) observed that over the Morteratsch Glacier in Switzerland (at 2100 m a.s.l) the daily mean albedo could be quite well simulated by expressing it as a function of snow age and h_s, while T did not play any significant role. On the other hand, *Brock et al.* (2000) observed that over another glacier in Switzerland (Haut Glacier d'Arolla, between 2572m and 3002m a.s.l.) snow albedo is best estimated from accumulated daily maximum 2-m air temperatures since snowfall, and noticed that Oerlemans and Knap's parameterization (1998) performed worse that all other schemes, including the constant albedo assumption. Over sea ice in the Baltic Sea, the evolution of the snow albedo during the spring melting season in 2004 was only little correlated with the 2-m air temperature (see Fig. 1), but instead it was almost completely controlled by the change in h_s (*Pirazzini et al.*, 2006). Indeed, also from other model inter-comparison studies emerged that during the snowmelt period h_s-dependent parameterizations perform better than T-dependent parameterizations (*Pedersen and Winther*, 2005; *Mölders et al.*, 2007). However, *Cheng et al.* (2007) concluded that, even if simple schemes of Pirazzini et al. (2006) tailored for local conditions gave the best simulation of the snow albedo evolution over the Baltic Sea, only the more sophisticated and physically-based albedo schemes could give the most accurate reproduction of the evolution of h_s, particularly at the beginning of the melting season. Over Greenland, the fundamental processes that should be accounted for to simulate the snow albedo were found to be the effect of aging, the snowpack densification and the melt-water percolation during the snowmelt (*Zuo and Oerlemans*, 1996).

From these studies emerges the enormous difficulty in producing a general scheme that simulates the albedo evolution in conditions of strong melting and strong albedo variations, when only few observable quantities are used as predictors, and the physical thermodynamic processes are not explicitly represented. The most complex parameterizations are superior to the simplest ones but still require a lot of improvements, and the uncertainties in the forcing variables in many cases compromise the performance of the parameterizations, with the result that no parameterization is significantly better than the others in simulating the whole-year cycle of snow/ice surface albedo (*Curry et al.*, 2001; *Pedersen and Winther*, 2005). Some general common features can be observed in the performance of the albedo parameterizations. In the Arctic, the modelled snow albedo has usually more temporal variability than the observed albedo (*Pedersen and Winther*, 2005; *Mölders et al.*, 2007), except for the simplest schemes with constant albedo. On the contrary over French Alps, where the alternation of snowfall and snow melting is present also during mid-winter, the albedo variability and the maximum daily average snow albedo (which according to observations is as high as 0.95) are underestimated by the models (*Boone and Etchevers*, 2001). In the Arctic, during the non-melting season (late autumn, winter, and early spring) the modelled snow albedo is most often too low, as it decreases at a faster rate or by a larger magnitude during the snow metamorphism than the observed albedo (*Pedersen and Winther*, 2005; *Mölders et al.*, 2007). This last error is a critical issue, as the accurate representation of the early spring snow albedo is a fundamental prerequisite to correctly simulate the late spring snowmelt and the evolution of the summer albedo (*Wyser et al.*, 2008).

Developing proper parameterizations for the albedo evolution is particularly difficult and critical during the spring melting season and the autumn refreezing season, because of the large variability in snow albedo and f_s during these periods (*Winther et al.*, 2002), and because the large availability of downward visible radiation, which enhances the snow-albedo feedbacks (*Hall*, 2004). In spring the Land Surface models overestimate the SWE (*Roesch*, 2006) and the Arctic terrestrial (or grid box mean) albedo compared to MODIS albedo products (*Slater et al.*, 2007). These errors are caused by differing dates of snowmelt, incorrect assessment of the fractional extent of vegetation masking and snow-covered areas, and overestimation of the snow albedo in the areas that are entirely snow covered. The last problem points directly to the incorrect albedo parameterization, while the first two problems concern the interaction among the parameterizations of albedo, vegetation masking, and f_s. The inter-model differences are largest when the SWE is small, that is at the beginning of the autumn and during the spring melting season (*Slater et al.*, 2001, *Roesch*, 2006). The amount of SWE directly drives the surface albedo, which rapidly increases as SWE increases, with different rates in different models (*Slater et al.*, 2001).

4.3 Some important missing dependencies in most of the present day albedo parameterizations

A problem faced when developing physically based albedo models is the paucity of complete datasets that include detailed observations of albedo together with snow properties. *Flanner and Zenner* (2006) developed a physically based snow albedo model which requires snow temperature, temperature gradient inside the snowpack, and ρ_s as prognostic variables. Their model suggested that the temperature gradient can be the most influential quantity on the albedo evolution, but it is not taken into account in the representation of snow aging in any general circulation model.

Only the most sophisticated albedo schemes (as BATS and LSM 1.0) are waveband dependent, and therefore can account for the albedo dependence on the ratio of diffuse to global radiation, which is mainly modulated by cloud cover. Snow albedo is significantly higher in the visible than in the near-infrared band, and snow aging effect has a much stronger impact over near-infrared than over visible wavelengths. *Roesch et al.* (2002) showed that the separate computation of visible and infrared albedo produce a broadband albedo over snow-covered forests in northern Eurasia and Canada that is 0.3 lower than without the distinction between band albedo. In regions undergoing strong snow and ice melting, the albedo dependence on the cloud cover fraction may be little or no significant compared to other quantities (see Table 1). Instead, over most of Antarctica, where snow metamorphism due to melting does not take place or it is irrelevant, cloud cover fraction is the main driver of the albedo variability (*Pirazzini*, 2004, *Van den Broeke et al.*, 2006).

Also the dependence of snow/ice albedo on θ is generally not accounted for, with the exception of the most sophisticated schemes. Usually snow and ice albedo observations in clear sky do not show the diurnal albedo cycle symmetric around noon predicted by the theory, because factors other than the variation in θ concur in shaping the diurnal albedo variation, as the snowmelt metamorphism or the alternation between crystal formation/precipitation during the night and successive sublimation during the day (*Pirazzini*, 2004). Thus, snow albedo follows more a steady decline with minimum in the afternoon, while ice albedo shows a quite strong decline in the morning and then keeps a rather constant value in the afternoon (*Pirazzini*, 2004; *Pirazzini et al.*, 2006). Over bare ice in Antarctica, for instance, an average albedo decrease by 31% from early morning to noon was observed (*Pirazzini*, 2004). Accounting for these diurnal albedo variations would be very important in order to correctly simulate the diurnal cycle of surface energy fluxes.

5. Influence of model structure and model parameterizations on the snow/ice albedo simulations

Similar snow albedo and f_s parameterizations can give quite different snow simulations in models with different structure and layering (*Slater et al.*, 2001). *Boone and Etchevers* (2001) compared three snow schemes with different structure and level

of sophistication by evaluating their performances in an Alpine site during two winter-to-spring seasons. They observed that the differences in modeled SWE were primarily related to contrasting turbulent flux parameterizations at the surface, which directly affected T and the degree of success in modeling the early to midwinter melt episodes. Indeed, T is very sensitive to model errors in the surface energy budget parameterization and in the representation of clouds (*Lynch et al.*, 1998). In general, the amount of energy available for snowmelt is the result of a small difference between radiative and turbulent fluxes. Therefore, the accurate computation of these fluxes is very important for the correct simulation of the snowpack before and after the start of the melting.

Slater et al. (2001) noticed a very large inter-model difference in T during winter as compared with summer. The reason is that the cooler is the modeled T, the cooler will become via longwave emission, creating a positive feedback in which the surface longwave budget is increasingly negative, determining a very strong stability that decouples the surface from the atmosphere. Thus, different schemes have different sensitivity to the downwelling longwave radiation (the coolest schemes having the highest sensitivity). Since snow age, ρ_s, snowmelt, and h_s are related to each other and to T, the winter and spring snowmelt and sublimation are very much affected by the model sensitivity to the downward longwave radiation.

The effect of differences in the snowpack model philosophy has been demonstrated by *Lynch et al.* (1998) and *Slater et al.* (2001). A bulk-layer model is not suitable for simulating the daily cycle of T as it filters out fast responses, but it may be suitable for long-timescale seasonal variations of heat flux. Instead, snowpack models based on the force-restore method allow a good estimation of T, but they force the soil temperature to follow the diurnal average surface temperature, therefore they are not suitable for hydrological studies, where instead a multilayered model should be preferred.

The vertical resolution of a thermodynamic sea ice model has a large impact on the simulation of the snow depth and on the onset of melting (*Slater et al.*, 2001; *Cheng et al.*, 2008). Moreover, *Cheng et al.* (2008) noticed that the increase of the model's vertical resolution decreases the sensitivity of snow and ice mass balance to changes in surface albedo. In climate models, also the horizontal resolution affects the albedo simulation over snow-covered regions: *Roesch* (2006) concluded that some of the IPCC-AR4 models underestimate the interannual variability of the snow cover area in Europe particularly during the spring snowmelt probably because of their too coarse horizontal resolution.

6.   *Impacts of the albedo parameterizations on the modeled future climate*

The results presented in the previous sections point to the necessity of further effort in improving the albedo parameterizations, so that they do not only reproduce the observed albedo variability and seasonal cycle, but also include the dependence on all relevant surface and atmospheric parameters. Indeed, even when the simplest parameterizations, tuned to represent local environments, result to be relatively good for

sea ice models, the lack of the suitable dependences with relevant parameters make them to fail in reproducing the snow/ice-albedo feedback and the radiative interaction with the atmosphere (*Curry et al.*, 2001; *Liu et al.*, 2007). Moreover, *Marshall and Oglesby* (1994) noticed that utilizing a physically based parameterization of snow albedo and f_s instead of a fixed parametric scheme had a tremendous impact on the simulation of the Northern Hemisphere glaciation, mostly because of the effect of feedbacks which were accounted for in the physically-based approach.

The strength of the modeled snow-albedo feedback on the temperature is proportional to the modeled mean effective snow albedo (the mean albedo of the snow-covered areas, including forests), because large effective snow albedos cause a large albedo contrast between snow-covered and snow-fee regions, and producing a correspondingly large albedo decrease when snow cover area decreases (*Qu and Hall*, 2007).

Hall (2004) and *Gorodetskaya et al.* (2008) showed that the snow- and ice-albedo feedback is indirectly modulated by long-term variations in clouds, which also have a positive feedback on temperature in the Arctic (*Soden et al.*, 2004; *Vavrus*, 2004), mostly due to an increase of the cloud longwave warming effect with increasing temperature. Therefore, the strong albedo sensitivity on cloud cover fraction observed on several Antarctic stations (*Pirazzini*, 2004; *Van den Broeke et al.*, 2006) points to the necessity of introducing the dependence on the ratio of diffuse to global radiation in the surface albedo schemes applied over Antarctica, in order to properly account for cloud- and albedo-feedback processes. In fact, the observed effect of clouds on the albedo represents a negative feedback on the near surface temperature, and it opposes the positive cloud feedback. If the albedo dependence on clouds is not included in model simulations, the cloud warming effect and the cloud positive feedback on the temperature are most probably overestimated.

The presence of black carbon at the snow surface triggers strong radiative feedbacks on the snow microphysics, snow albedo, and T, insomuch as black carbon over snow has recently been claimed to be one of the most important contributor to the global warming, being twice as effective as CO2 in altering the global temperature (*Hansen and Nazarenko*, 2004; *Hansen et al.*, 2005). The reason for this large response of climate to black carbon over the snow were identified in the amplification of the snow-albedo feedback and in the relative stability of the atmospheric temperature profile at high latitudes, which tend to confine the thermal response to the surface. In spite of these recent results, the effect of soot and black carbon over the snow is rarely accounted for in snow albedo schemes. *Flanner et al.* (2007) have recently demonstrated that accounting for the black carbon deposition on the snow noticeably reduce the Arctic annual mean surface albedo, accelerating the snowmelt and greatly amplifying the snow-albedo feedback on the climate. And jet, their experiment did not account for the effect of other aerosols, as mineral dust, volcanic ash, brown carbon, and marine sediment in sea-ice.

7.   Conclusions

The general recommendation given by many authors to improve the snow and ice albedo parameterization is to orient toward more physically-based schemes, which more closely relate the evolution of the albedo to the evolution of the snow grain structure in response to the energy exchanges with the atmosphere. The inclusion of the albedo dependence on r and ρ_s, on the vertical temperature gradient in the snowpack, on the accumulation of impurities, on θ, and on the ratio of diffuse to global radiation has a demonstrated positive impact on the accuracy of present climate simulations. Other aspects that are presently missing in the albedo formulations but have a significant impact on the albedo results are also the effect of drifting snow, of wind-driven snow aging, and of snow redistribution (*Lynch et al.*, 1998).

The reasons why very simple schemes give on average performances comparable to the more physically-based schemes when compared to the observed albedo are mainly two. The first reason is the lack of suitably complete and accurate forcing data for the model (above all, precipitation and impurity content). The second reason is the model's oversimplification of the surface turbulent fluxes and of the vertical structure of the snowpack; this strongly affects snow melting and temperature, which are among the main drivers of the snow/ice albedo and f_s parameterizations. Because of these problems, in climate studies over long time scales the increase in sophistication of the albedo scheme may also lead to drastic simulation errors, when small inaccuracies are integrated in time and amplified by feedback mechanisms.

In single-column applications and when the modeling strategy allows large computational time, snow/ice albedo should be modeled as a function of the primary physical parameters effecting the albedo (grain size, shape, impurities, surface roughness, wavelength), and the model's vertical resolution should be high enough to allow a proper discrimination of the layering inside the snowpack. In other applications that require fast model's runs (as in NWP and climate modeling) such a detailed computation is not feasible. Therefore, the relationship between albedo, snow grain structure and energy flux through the surface has to be simplified by parameterizing the albedo via waveband-dependent coefficients and temperature/wind speed/snow mass-dependent equations.

To develop more accurate and physically-based snow albedo parameterizations it is of paramount importance to carry out field experiments with simultaneous measurements of albedo and snow properties (r and ρ_s, vertically resolved temperature, impurity concentration) at high temporal resolution. Such a complete datasets are extremely rare at the present time. However, during two recent Finnish Antarctic expeditions at the research station Aboa, the time series of albedo and snow properties has been measured with very high temporal resolution, providing an excellent dataset to test and improve snow albedo parameterizations. Moreover, a field campaign with extensive measurements of snow properties and albedo measurements is going on in a snow-covered forested region in Sodankylä, in northern Finland. The dataset that will be

collected is expected to give more insight on the complicated and very actual issue of the albedo evolution in snow-covered forests during the melting season.

References

Barker, H.W., A. Marshak, W. Szyrmer, A. Trishchenko, J.-P. Blanchet and Z. Li, 2002. Inference of cloud optical depth from aircraft-based solar radiometric measurements, *J. Atmos. Sci.*, **59**, 2093–2111.

Benner, T.C., J.A. Curry and J.O. Pinto, 2001. Radiative transfer in the summertime Arctic, *J. Geophys. Res.*, **106**, 15173–15183.

Bonan, G.B., 1996. A Land Surface Model (LSM Version 1.0) for ecological, hydrological, and atmospheric studies: technical description and user's guide, *Tech. Rep. NCAR/TN-417+STR*, National Center for Atmospheric Research, Boulder,CO, 150 pp.

Bony, S., R. Colman, V.M. Kattsov, R.P. Allan, C.S. Bretherton, J.-L. Dufresne, A. Hall, S. Hallegatte, M.M. Holland, W. Ingram, D.A. Randall, B.J. Soden, G. Tselioudis, M.J. Webb, 2006. How well do we understand and evaluate climate change feedback processes? *J. Clim.*, **19**, 3445–3482.

Boone, A. and P. Etchevers, 2001. An intercomparison of three snow schemes of varying complexity coupled to the same Land Surface Model: local scale evaluation in an Alpine site, *J. Hydrometeorol.*, **2**, 374–394.

Broch, B.W., I.C. Willis and M.J. Sharp, 2000. Measurement and parameterization of albedo variations at Haut Glacier d'Arolla, Switzerland, *J. Glaciol.*, 46, 675–688.

Cheng, B., A. Riihelä, K. Andersson and T. Manninen, 2007. The Surface Albedo Product (SAL) of CM-SAF in Modeling of Sea Ice Mass Balance, *Joint 2007 EUMETSAT Meteorological Satellite Conference and the 15th Satellite Meteorology & Oceanography Conference of the American Meteorological Society*, Amsterdam, The Netherlands, 24–28 September 2007

Cheng, B., T. Vihma, R. Pirazzini, M.A. Granskog, 2006. Modelling of superimposed ice formation during the spring snowmelt period in the Baltic Sea, *Annals of Glaciol.*, **44**, 139–146.

Cheng, B., Z. Zhang, T. Vihma, M. Johansson, L. Bian, Z. Li and H. Wu, 2008. Model experiments on snow and ice thermodynamics in the Arctic Ocean with CINARE 2003 data, *J. Geophys. Res.*, **113**, C09020, doi:10.1029/2007JC004654.

Collins, W.D., C. Bitz, B.A. Boville, B. Briegleb, Y. Dai, J.J. Hack, J.T. Kiehl, S.-J. Lin, J.R. Mccaa, P. J. Rasch, R. B. Rood, D. L. Williamson and M. Zhang, 2002. Description of the NCAR Community Atmosphere Model (CAM2), http://www.ccsm.ucar.edu/models/atm-cam/docs/cam2.0/description/index.html.

Cox, P.M., R.A. Betts, C. B. Bunton, R.L.H. Essery, P.R. Rowntree and J. Smith, 1999. The impact of new land surface physics on the GCM simulation of climate and climate sensitivity, *Clim. Dyn.*, **15**, 183–203.

Curry, J.A., J.L. Schramm, D.K. Perovich and J.O. Pinto, 2001. Applications of SHEBA/FIRE data to evaluation of snow/ice albedo parameterizations, *J. Geophys. Res.*, **106** (D14), 15345–15355.

Dickinson, R.E., A. Henderson-Sellers and P.J. Kennedy, 1993. Biosphere-Atmosphere Transfer Scheme (BATS) Version le as Coupled to the NCAR Community Climate Model, *Tech. Rep. NCAR/TN-387+STR*, National Center for Atmospheric Research, Boulder,CO, 174 pp.

Douville, H., J.-F. Royer, J.-F. Mahfouf, 1995. A new snow parameterization for the Météo-France climate model, *Clim. Dyn.*, **12**, 21–35.

ECMWF, 2007. IFS documentation CY31r1, http://www.ecmwf.int/research/ifsdocs /CY31r1/index.html.

Flanner, M.G. and C.S. Zender, 2006. Linking snowpack microphysics and albedo evolution, *J. Geophys. Res.*, **111**, D12208, doi:10.1029/2005JD006834.

Flanner, M.G., C.S. Zender, J.T. Randerson and P.J. Rasch, 2007. Present-day climate forcing and response from black carbon in snow, *J. Geophys. Res.*, **112**, D11202, doi:10.1029/2006JD008003.

Gordon, C., C. Cooper, C.A. Senior, H. Banks, J.M. Gregory, T.C. Johns, J.F.B. Mitchell and R. Wood, 2000. The simulation of SST, sea ice extents nad ocean heat transports in a version of the Hadley Centre coupled model without flux adjustments, *Climate Dyn.*, **16**, 147–168.

Gorodetskaya, I.V., L.-B. Tremblay, B. Liepert, M.A. Cane and R.I. Cullather, 2008. The influence of cloud and surface properties on the Arctic Ocean shortwave radiation budget in coupled models, *J. Clim.*, **21**, 866–882.

Grenfell, T.C. and G.A. Maykut, 1977. The optical properties of ice and snow in the Arctic basin, *J.Glaciol.*, **18**, 445–463.

Grenfell, T.C. and D.K. Perovich, 2004. Seasonal and spatial evolution of albedo in a snow-ice-land-ocean environment, *J. Geophys. Res.*, **109**, C01001, doi:10.1029/2003JC001866.

Greuell, W. and T. Konzelmann, 1994. Numerical modeling of the energy balance and the englacial temperature of the Greenland Ice Scheet. Calculations for the ETH-Camp location (West Greenland, 1155 n a.s.l.), *Global Planet. Change*, **9**, 91–114.

Hall, A., 2004. The role of surface albedo feedback in climate, *J. Clim.*, **17**, 1550–1568.

Hall, A. and X. Qu, 2006. Using the current seasonal cycle to constrain snow albedo feedback in future climate change, *Geophys. Res. Lett.*, **33**, L03502, doi:10.1029/2005GL025127.

Hansen, J., et al., 2005. Efficacy of climate forcing, *J. Geophys. Res.*, **110**, D18104, doi:10.1029/2005JD005776.

Hansen, J. and L. Nazarenko, 2004. Soot climate forcing via snow and ice albedo, *Proc. Natl. Acad. Sci. U.S.A.*, **101**, 423–428.

Køltzow, M., 2007. The effect of a new snow and sea ice albedo scheme on regional climate model simulations, *J. Geophys. Res.*, **112**, D07110, doi:10.1029/2006JD007693.

Laine, V., 2008. Antarctic ice sheet and sea ice regional albedo and temperature change, 1981–2000, from AVHRR Polar Pathfinder data, *Remote Sens. Env.*, **112**, 646–667.

Levis, S., G.B. Bonan and P.J. Lawrence, 2007. Present-day springtime high-latitude surface albedo as a predictor of simulated climate sensitivity, *Geophys. Res. Lett.*, **34**, L17703, doi:10.1029/2007GL030775.

Liu, J., Z. Zhang, J. Inoue and R.M. Horton, 2007. Evaluation of snow/ice albedo parameterizations and their impacts on sea ice simulations, *Int. J. Climatol.*, **27**, 81–91.

Los, S.O., G.J. Collatz, P.J. Sellers, C.M. Malmström, N.H. Pollack, R.S. DeFries, L. Bounoua, M.T. Parris, C.J. Tucker and D.A. Dazlich, 2000. A global 9-year biophysical land surface dataset from NOAA AVHRR data. *J. Hydrometeorol.*, **1**, 183–199.

Loth, B. and H.-F. Graf, 1998. Modeling the snow cover in climate studies – 1. Long-term integrations undr different climatic conditions using a multilayered snow-cover model, *J. Geophys. Res.*, **103**(D10), 11313–11327.

Lynch, A.H., D.L. McGinnis and D. Bailey, 1998. Snow-albedo feedback and the spring transition in a regional climate system model: influence of land surface model, *J. Geophys. Res.*, **103**(D22), 29037–29049.

Marshall, S. and R.J. Oglesby, 1994. An improved snow hydrology for GCMs. Part 1: snow cover fraction, albedo, grain size, and age, *Clim. Dyn.*, **10**, 21–37.

Masson, V., Champeaux, J.-L., Chauvin, F., Meriguet, C. and Lacaze, R., 2003. A global database of land surface parameters at 1-km resolution in meteorological and climate models. *J. Climate* **16**(9), 1261–1282.

Mölders N., H. Luijting and K. Sassen, 2007. Use of atmospheric radiation measurement program data from Barrow, Alaska, for evaluation and development of snow-albedo parameterizations, *Meteorol. Atmos. Phys.*, doi: 10.1007/s00703-007-0271-6.

Niu G.-Y and Z.-L. Yang, 2007. An observational-based formulation of snow cover fraction and its evaluation over large North America river basins, *J. Geophys. Res.*, **112**, D21101, doi:10.1029/2007JD008674.

Oerlemans, J. and W.H. Knap, 1998. A 1 year record of global radiation and albedo in the ablation zone of Morteratschgletscher, Switzerland, *J. Glaciol.*, **44**, 1998.

Oleson, K.W. et al., 2004. Technical Description of the Community Land Model (CLM), *Tech. Rep. NCAR/TN-461+STR*, National Center for Atmospheric Research, Boulder,CO, 174 pp.

Parish, T.R., 1988. Surface winds over the Antarctic continent: a review, *Rev. Geophys.*, **26**, 169–180.

Pedersen, C.A. and J.-G. Winther, 2005. Intercomparison and validation of snow albedo parameterization schemes in climate models, *Clim. Dyn.*, **25**, 351–362.

Pirazzini, R., T. Vihma, J. Launiainen and P. Tisler, 2002. Validation of HIRLAM boundary-layer structures over the Baltic Sea, *Bor. Environ. Res.*, **7**, 211–218.

Pirazzini, R., 2004. Surface albedo measurements over Antarctic sites in summer, *J. Geopys. Res.,* **109**, D20118, doi:10.1029/2004JD004617.

Pirazzini, R., T. Vihma, M.A. Granskog and B. Cheng, 2006. Surface albedo measurements over sea ice in the Baltic Sea during the spring snowmelt period. *Annals of Glaciol.*, **44**, 7–14.

Pirazzini, R. and P. Räisänen, 2008. A method to account for surface albedo heterogeneity in single column radiative transfer calculations under overcast conditions, *J. Geopys. Res.*, **113**, D20108, doi:10.1029/2008JD009815.

Qu, X. and A. Hall, 2007. What control the strength of snow-albedo feedback?, *J. Clim.*, **20**, 3971–3981.

Rasmus, K., J. Ehn, M. Granskog, E. Kärkäs, M. Leppäranta, A. Lindfors, A. Pelkonen and S. Rasmus, 2002. Optical measurements of sea ice in the Gulf of Finland, *Nordic Hydrology*, **33**, 207–226.

Robock, A., 1983. Ice and snow feedbacks and the latitudinal and seasonal distribution of climate sensitivity*, J. Atmos. Sci.*, 40, 986–997.

Roeckner, E., Arpe, K., Bengtsson, L., Christoph, M., Claussen, M., Dümenil, L., Esch, M., Giorgetta, M., Schlese, U. & Schulzweida, U., 1996. The atmospheric general circulation model ECHAM-4: model description and simulation of present-day climate. *Max-Planck Institute for Meteorology Report,* No. **218**, Hamburg, Germany, 90pp.

Roeckner, E., G. Bäuml, L. Bonaventura, R. Brokopf, M. Esch, M. Giorgetta, S. Hagemann, I. Kirchner, L. Kornblueh, E. Manzini, A. Rhodin, U. Schlese, U. Schulzweida and A. Tompkins, 2003. The atmospheric general circulation model ECHAM-5: model description. *Max-Planck Institute for Meteorology Report* No. **349**, Hamburg, Germany, 140pp.

Roesch, C.A., 2000. Assessment of the land surface scheme in climate models with focus on surface albedo and snow cover, Zurchen Klima-Schriften 78, ETH Geographischen Institut, Zurich.

Roesch, C.A., H. Gilgen, M. Wild and A. Ohmura, 1999. Assessment of GCM simulated snow albedo using direct observations, *Climate Dynamics*, **15**, 405–418.

Roesch, C.A., M. Wild, R. Pinker and A. Ohmura, 2002. Comparison of spectral surface albedos and their impact on the general circulation model simulated surface climate, *J. Geopys. Res.,* **107**(D14) doi:10.1029/2001JD000809.

Roesch, A., C. Schaaf and F. Gao, 2004. Use of Moderate-Resolution Imaging Spectroradiometer bidirectional reflectance distribution function products to enhance simulated surface albedos, *J. Geopys. Res.,* **109**, D12105, doi:10.1029/2004JD004552.

Roesch, A., 2006. Evaluation of surface albedo and snow cover in AR4 coupled climate models, *J. Geopys. Res.,* **111**, D15111, doi:10.1029/2005JD006473.

Ross, B.R. and J.E Walsh, 1987. A comparison of simulated and observed fluctuations in summertime Arctic surface albedo, *J. Geophys. Res.*, **92**, 13115–131125.

Rutter, N. et al., 2009. Evaluation of forest snow processes models (SnowMIP2), *J. Geopys. Res.*, **114**, D06111, doi:10.1029/2008JD011063.

Slater, A.G., T.J. Bohn, J.L. McCreight, M.C. Serreze and D.P. Lettenmaier, 2007. A multimodel simulation of pan-Arctic hydrology, *J. Geopys. Res.*, **112**, G04S45, doi:10.1029/2006JG000303.

Slater, A.G., et al., 2001. The representation of snow in Land Surface Schemes: results from PILPS 2(d), *J. Hydrometeorol.*, **2**, 7–25.

Soden, B.J., A.J. Broccoli and R.S. Hemler, 2004. On the use of cloud forcing to estimate cloud feedback, *J. Clim.*, **19**, 3661–3665.

van den Broeke, M., C. Reijmer, D. Van As and W. Boot, 2006. Daily cycle of the surface energy balance in Antarctica and the influence of clouds, *Int. J. Climatol.*, **26**, 1587–1605.

van den Hurk, B. and P. Viterbo, 2003. The Torne-Kalix PILPS 2(e) experiment as a test bed for modifications to the ECMWF land surface scheme, *Global Planet. Change*, **38**, 165–173.

Vavrus, S., 2004. The impact of cloud feedbacks on Arctic climate under greenhouse forcing, *J. Clim.*, **17**, 603–615.

Viterbo, P. and A.K. Betts, 1999. Impact on ECMWF forecasts of changes to the albedo of the boreal forests in the presence of snow, *J. Geophys. Res.*, **104**(D22), 27803–27810.

Warren, S.G., 1982. Optical properties of snow, *Rev. Geophys.*, **20**, 67–89.

Winther, J.-G., F. Godtliebsen, S. Gerland, P.E. Isachsen, 2002. Surface albedo in Ny-Ålesund, Svalbard: variability and trends during 1981–1997, *Global Planet. Change*, **32**, 127–139.

Wyser, K., C.G. Jones, P. Du, E. Girard, U. Willen, J. Cassano, J.H. Christensen, J.A. Curry, K. Dethloff, J.-E. Haugen, D. Jacob, M. Kølzov, R. Laprise, A. Lynch, S. Pfeifer, A. Rinke, M. Serreze, M.J. Shaw, M. Tjerrnström and M. Zagar, 2008. An evaluation of Arctic cloud and radiation processes during the SHEBA year: simulaton results from eight Arctic regional climate models, *Clim. Dyn.*, **30**, 203–223.

Yang, Z.-L., R.E. Dickinson, A. Robock and K.Y. Vinnikov, 1997. Validation of the snow submodel of the Biosphere-Atmosphere Transfer Scheme with Russian snow cover and meteorological observational data, *J. Clim.*, **10**, 353–373.

Zuo, Z. and J. Oerlemans, 1996. Modelling albedo and specific balance of the Greenland ice sheet: calculations for the Søndre Strømfiord transect, *J. Glaciol.*, **42**, 1996.

List of symbols

Age = Days after snowfall

F = Incident irradiance (Wm^{-2}λ^{-1})

f_s = Snow cover fraction

h_s = SWE/ρ_s = Snow depth (m)

I = Reflected radiance (Wm^{-2}sr^{-1}λ^{-1})

r = Snow grain radius (m)

SWE = Snow water equivalent (Kg m^{-2})

S_n = SWE/ρ_w = Snow water equivalent expressed in water depth (m)

Sw = Shortwave irradiance (Wm^{-2})

T = Surface temperature (°C)

z = Surface roughness length (m)

α_b = Abedo of snow-free surface

α_i = Ice albedo

α_{max} = Upper limit of snow albedo

α_{min} = Lower limit of snow albedo

α_s = Snow albedo

θ = Solar zenith angle (degrees)

λ = Wavelength

μ = Cosine of zenith angle

ρ_s = Snow density (Kg m^{-3})

ρ_{snew} = Density of new snow (Kg m^{-3})

ρ_w = Water density (Kg m^{-3})

ϕ = Azimuth angle

List of acronyms

ARPEGE= Action de Recherche Pétite Echelle Grande Echelle

BATS = Biosphere-Atmosphere Transfer Scheme

CAM2 = NCAR Community Atmosphere Model – Version 2

CCSM = NCAR Community Climate System Model

CLM = Community Land Model

ECHAM4-5 = European Centre/Hamburg general circulation model (Versions 4 and 5)

ECMWF = European Centre for Medium-Range Weather Forecasts

GCM = General Circulation Model

HadCM3 = Met Office's Third Hadley Centre Coupled Ocean-Atmosphere GCM

HIRLAM5= High Resolution Limited Area Model (version5)

IPCC-AR4 models = Climate models contributing to the Fourth Assessment Report by the International Panel on Climate Change

ISBA = Interaction between Soil, Biosphere and Atmosphere

LSM1.0 = Land Surface Model – Version 1.0

NCAR = United States National Center for Atmospheric Research

NWP = Numerical Weather Prediction